Zhou, You et al.

Article

Desulphurization of coals of different ranks in the presence of slimes by reverse flotation

Energy Reports

Provided in Cooperation with:
Elsevier

Suggested Citation: Zhou, You et al. (2019) : Desulphurization of coals of different ranks in the presence of slimes by reverse flotation, Energy Reports, ISSN 2352-4847, Elsevier, Amsterdam, Vol. 5, pp. 1316-1323, https://doi.org/10.1016/j.egyr.2019.09.003

This Version is available at:
https://hdl.handle.net/10419/243672

Energy Reports 5 (2019) 1316–1323

Contents lists available at ScienceDirect

Energy Reports

journal homepage: www.elsevier.com/locate/egyr

Research paper

Desulphurization of coals of different ranks in the presence of slimes by reverse flotation

You Zhou [a,b], Boris Albijanic [b,*], Bogale Tadesse [b,*], Yuling Wang [a], Jianguo Yang [a], Xiangnan Zhu [c]

[a] Key Laboratory of Coal Processing and Efficient Utilization of Ministry of Education, School of Chemical Engineering and Technology, China University of Mining and Technology, Xuzhou 221116, Jiangsu, China
[b] Western Australian School of Mines: Minerals, Energy and Chemical Engineering, Curtin University, Australia
[c] College of Chemical and Environmental Engineering, Shandong University of Science and Technology, Qingdao, Shandong 266590, China

ARTICLE INFO

Article history:
Received 5 February 2019
Received in revised form 9 August 2019
Accepted 5 September 2019
Available online xxxx

Keywords:
Desulphurization
Sub-bituminous coal
Meta-bituminous coal
Pyrite
De-sliming
Flotation

ABSTRACT

In this paper, the flotation separation of pyrite from sub-bituminous and meta-bituminous coals in the presence of slimes was investigated. The sub-bituminous coal and the meta-bituminous coal have significant differences in their surface properties compared with pyrite. The flotation experiments were performed in the presence of potassium amyl xanthate (PAX) collector. The adsorption of PAX on pyrite was significant while that on the coal surfaces was negligible. The recovery of pyrite from sub-bituminous coal increased by 55% when the concentration of PAX increased from 1×10^{-4}mol/L to 5×10^{-4}mol/L. Similarly, pyrite recovery from the meta-bituminous coal increased by up to 60% for the coarser size fraction upon increasing PAX concentration from 1×10^{-4}mol/L to 5×10^{-4}mol/L. Before the de-sliming process, the flotation recovery of pyrite increased with decreasing coal particle size whereas the opposite is true for pyrite grade. Desliming reduced the adsorption amount of PAX on pyrite by more than 50% because of the removal of fine particles that would otherwise be available for adsorption. Desulphurization of fine coal appears to be challenging probably due to the increased entrainment of fine coal particles during pyrite flotation. The de-sliming process increased pyrite grade by >20% for the meta-bituminous coal and by 10% for the sub-bituminous coal. The results suggest that excessive collector consumption by fine particles and slimes, and entrainment are the main challenges in separating pyrite from coal particles.

1. Introduction

Inorganic sulphur is present in many coals in the form of pyrite, marcasite, iron sulphates (e.g., $FeSO_4$) and elemental form (Eligwe, 1988). The sulphur in coals is highly undesirable because it reduces its economic value and results in SO_2 emission into the environment during coal combustion (Fuerstenau et al., 2007), and the SO_2 generated in this process is one of the most harmful air pollutants and can chemically react with rainwater to cause acid rain (Ga Siorek, 1997; Jha et al., 2011). Pyritic sulphur present in tailings can be oxidized in the presence of oxygen and water, and produces sulphuric acid, which leads to acid mine drainage (AMD). Subsequently, the AMD is the main cause for the leaching of toxic elements present in the tailings which has become a critical environmental concern (Akcil and Koldas, 2006). Therefore, the removal of sulphide minerals prior to coal utilization (desulphurization) has significant economic and environmental implications, and enhances the sustainability of coal mining operations.

Desulphurization methods for the removal of inorganic sulphur include gravity separation (e.g., use of hydrocyclones), magnetic separation and flotation (Demirbas and Balat, 2004). Microbial (Eligwe, 1988) and chemical desulphurization methods such as washing with alkaline solutions or organic and inorganic acids are practised to remove organic sulphur (Demirbas and Balat, 2004). Gravity separation methods are usually employed in coal beneficiation due to the significantly lower density of coal (e.g., 1 – 1.5 g/cm^3) in comparison with the density of gangue minerals to be rejected (> 5 g/cm^3). Thus, dense medium cyclones (Wang et al., 2017; Dou et al., 2015), fluidized dry beneficiation (Tang, 2017) and jigs (Kumar and Venugopal, 2017) are extensively used in the processing of coarse coal particles (> 0.5 mm) due to their superior performance over other methods. However, the efficiency of gravity separation methods declines significantly in the presence of high proportion of ultrafine particles and slimes. In such case, froth flotation is widely used for fine coal cleaning

* Corresponding authors.
E-mail addresses: boris.albijanic@curtin.edu.au (B. Albijanic), bogale.tadesse@curtin.edu.au (B. Tadesse).

https://doi.org/10.1016/j.egyr.2019.09.003

and upgrading (Kawatra and Eisele, 1997), even in cases where coal has undergone surface oxidation (Xia et al., 2015a; Chen et al., 2017a).

It is well known that high rank coal is naturally hydrophobic and is floatable in neutral pH conditions. The fine pyrite present in the pulp can also be naturally hydrophobic depending on chemical conditions and can float with coal and/or recovered by entrainment in the froth phase at fine particle sizes (Kawatra and Eisele, 1997; Çınar, 2009), which makes fine coal beneficiation challenging. Surface oxidation of both coal and pyrite can significantly impact on the success of coal beneficiation by flotation (Fuerstenau et al., 1987). Another challenge is the poor floatability of low rank coals due to the presence of various hydrophilic surface functional groups on coal (Ye et al., 1988; Chen et al., 2017b), and the presence of floatable gangue (Xia et al., 2016; Xia and Yang, 2013). Thus, low rank coals are difficult to float even at high collector dosages in comparison with high rank coals which are floatable even in the absence of collectors (Fiedler and Bendler, 1992).

When coals containing pyrite is weathered, oxidation of pyrite leads to the formation of elemental sulphur on pyrite surface which makes pyrite naturally hydrophobic (Fuerstenau et al., 1990). The formation of elemental sulphur can proceed in one of the following two reactions (Kawatra and Eisele, 1997):

$$2Fe^{3+}(aq) + FeS_2(s) \rightarrow 3Fe^{2+}(aq) + 2S(s) \quad (1)$$

$$FeS_2 + 3H_2O \rightarrow Fe(OH)_3 + 2S^{\circ} + 3H^{+} + 3e^{-} \quad (2)$$

The above reactions (Eqs. (1) and (2)) suggest that the presence of fine pyrite in coal can complicate the beneficiation of low rank or weathered coal by flotation. Additionally, when slimes are present in coal, slime coating on the coal surface by van der Waals attraction could lead to poor coal cleaning performances in saline water (Wang et al., 2013) and presence of clay (Oats et al., 2010; Ni et al., 2018). Although the flotation behaviour of pyrite is well established, there is limited information on the separation of pyrite from coals of various ranks, especially in the presence of slimes. Thus, the present article investigates the separation of pyrite from the sub-bituminous coal (i.e. low rank coal) and that from the meta-bituminous coals (i.e. high rank coal) before and after de-sliming process.

2. Materials and methods

2.1. Materials

Sub-bituminous coal and meta-bituminous coal samples were collected from Shanxi province in China. The coal samples were crushed and screened to four different size fractions (−500 + 250 μm, −250 + 125 μm, −125 + 74 μm and −74 + 45 μm). The proximate analyses of sub-bituminous coal and meta-bituminous coal samples were moisture content of 6.1% and 1.5%, volatile matter content of 26.5% and 18.3%, ash content of 22.9% and 26.9%, fixed carbon content of 44.4% and 53.3% and total sulphur content of 0.63% and 0.39%, respectively. The contact angles of sub-bituminous coal and meta-bituminous coal samples used in this study are 41° and 79°, respectively (Zhou et al., 2019a). A more detailed characterization of the two coal samples using XRD, FTIR, XPS and SEM was published by the authors elsewhere (Zhou et al., 2019b,a). High purity pyrite sample (over 95% purity) used in this study was obtained from Navajun, La Rioja in Spain. The pyrite sample was dry ground with a ceramic mortar and pestle to obtain four size fractions (−300 + 212 μm,−212 + 150 μm, −150 + 75 μm and −75 + 38 μm). Potassium amyl xanthate (PAX) and copper sulphate from Chem-supply were used as a collector and activator for pyrite, respectively. Methyl isobutyl carbinol (MIBC) from Orica Australia was used as a frother. Starch (Chem-supply) was used as coal depressant for selective flotation of pyrite. All reagents were of analytical grade. Double distilled water with a resistivity of 18.2 MΩ was used for the preparation of all solutions.

2.2. Methods

The size distribution of pyrite and coal samples was characterized by Malvern Mastersizer 3000. The adsorption of PAX on pyrite and the two coals was characterized with the UV–visible spectrophotometer (PerkinElmer, Inc., USA). Desliming was conducted by adding a known amount of coal or pyrite into a beaker containing double distilled water. The mixture was then kept in an ultrasonic bath for 2 mins, and the supernatant solution was decanted. This sonication was repeated by adding more water until a clear supernatant solution was achieved. For each adsorption test, 0.5 g de-slimed samples were conditioned with 50 ml PAX solutions for 5 min and centrifuged at 3100 r/min. Then, the solutions were filtered to minimize the effect of fine particles, and adsorption measurements were conducted on the filtrates. All measurements were repeated at least three times. The adsorption densities of PAX on coal and pyrite were determined by the solution depletion method (Mukerjee and Mukerjee, 1962). In this method, the UV-spectra was firstly obtained based on the known concentrations of PAX solutions, which indicated that the maximum absorbance for different PAX solutions occurred at a wavelength of about 301 nm which is in agreement with the literature data (Agorhom et al., 2014). The absorbance values of the residual PAX solutions after adsorption experiments were determined, and the PAX concentrations were calculated using a calibration curve.

Zeta potential measurements were conducted using a Zetasizer (Malvern Nano Z, UK) to confirm the differences in surface chemistry between pyrite, and sub-bituminous and meta-bituminous coals in the presence of PAX collector. A 0.05 g samples of pyrite and coal were conditioned in 100 ml of deionized water for 5 min. The coarse particles were then allowed to settle down, and the supernatant solution containing fine particles was used for the zeta potential measurements. The solution was poured into a special capillary cell and the zeta potential was recorded using a Malvern Panalytical software. Each test was repeated at least four times.

Micro-flotation tests were carried out to investigate the flotation separation efficiency of pyrite from sub-bituminous and meta-bituminous coal samples before and after de-sliming. The desliming process was conducted by the ultrasonic bath. In each flotation test, 1 g pure pyrite particles were fully mixed with 1 g coal particles. Before each flotation tests, the samples before or after de-sliming process were conditioned for 5 min in the presence of PAX collector (1×10^{-4} mol/L or 5×10^{-4} mol/L), starch depressant (3 kg/t), $CuSO_4$ activator (20 g/t) and MIBC frother. The conditioned pulp was transferred into a 300 mL microflotation column, which was used to conduct the flotation experiments. The air flow rate was set to 0.5 L/min. The flotation experiments were repeated three times with a maximum error of less than 5%. The flotation performance was characterized by recovery and grade of pyrite determined by sulphur analysis using LECO SC632 Sulphur Analyser.

3. Results and discussion

3.1. Particle size distribution analysis

The particle size distribution (PSD) of the two coals and pyrite samples were determined to establish the slime deportment with

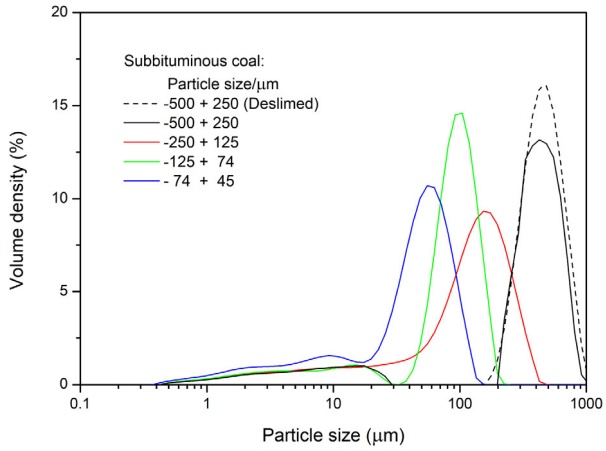

(a)

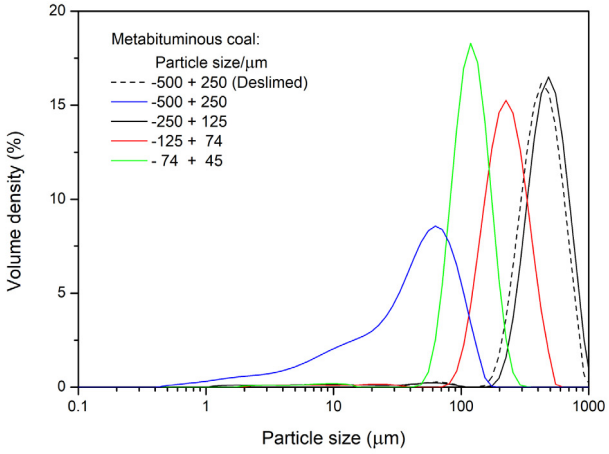

(b)

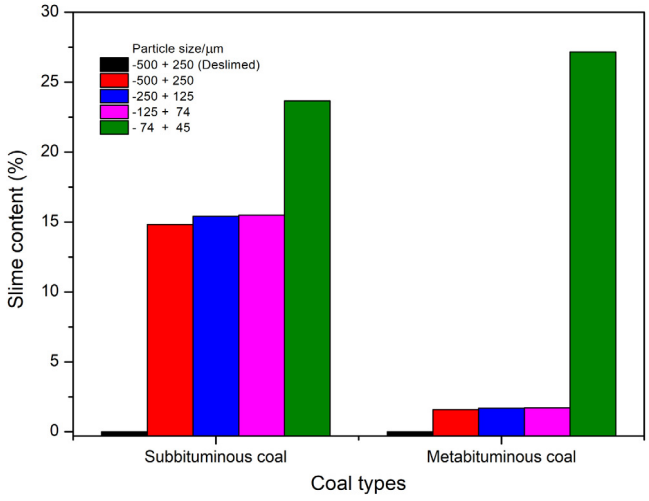

(c)

Fig. 1. Particles size distribution of (a) sub-bituminous coal and (b) meta-bituminous coal, and (c) their corresponding slime content at various particle size fractions.

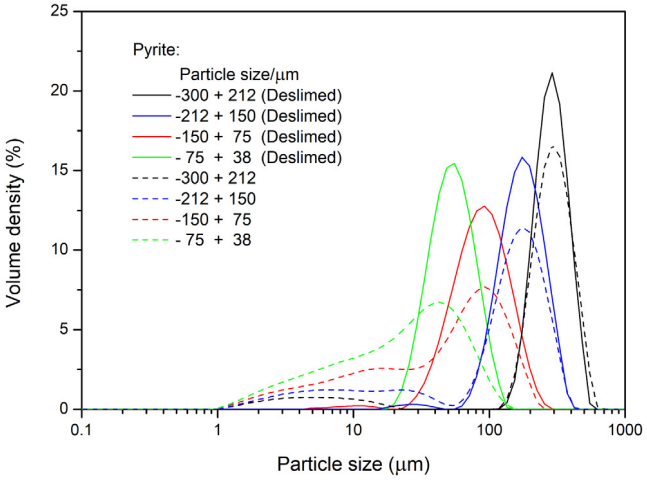

(a)

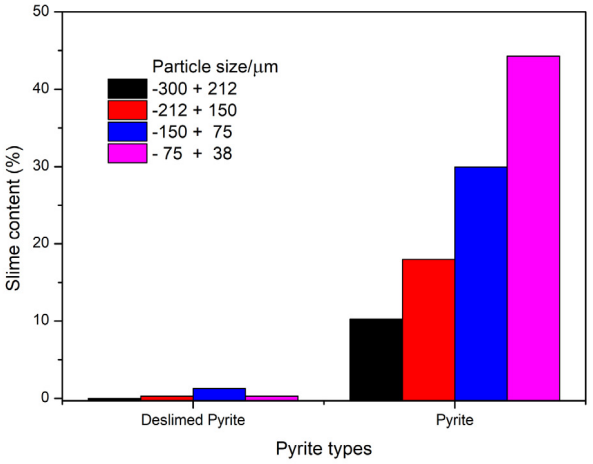

(b)

Fig. 2. Particle size distribution of pyrite (a) before and after the de-sliming process. and (b) corresponding slime content at various particle size fractions.

particle size, and to investigate the effect of particle size on desulphurization of coal. The PSD was determined by using a Mastersizer 3000 laser particle sizer (Malvern, UK). Fig. 1(a) shows the particle size distribution of the sub-bituminous coal, while Fig. 1(b) shows that of the meta-bituminous coal sample. The slime content of both coal samples is shown in Fig. 1(c), which implies that the slime content of the coal samples increased with decreasing particle size. The highest slime content was observed in the fine particle size fraction ($-74 + 45$ μm) for both the sub-bituminous coal and meta-bituminous coal and was recorded as 23.68% and 27.16%, respectively.

Fig. 2(a) and (b) show the particle size distribution of pyrite before and after de-sliming and the corresponding slime contents, respectively. It can be seen that the slime content increases with decreasing particle size, with the highest slime content of 44.28% obtained in the $-74 + 45$ μm size fraction.

3.2. UV–visible analysis

Collector adsorption plays a key role in flotation, and is often directly proportional to flotation recovery. The amount of

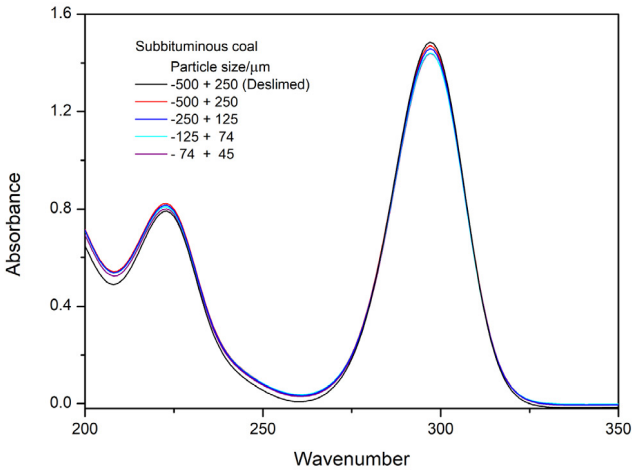

(a)

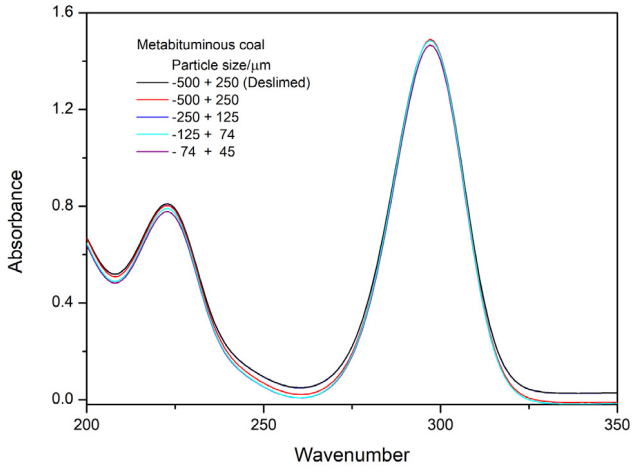

(b)

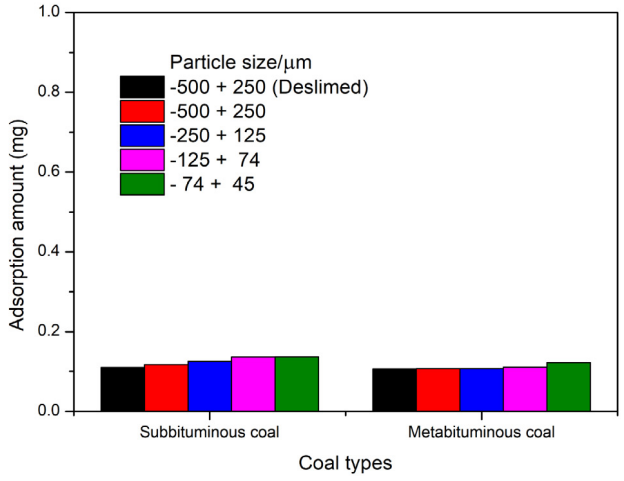

(c)

Fig. 3. The UV-visible absorbance of (a) sub-bituminous coal and (b) meta-bituminous coal and (c) their corresponding adsorption amount in 10^{-4} mol/L PAX solution.

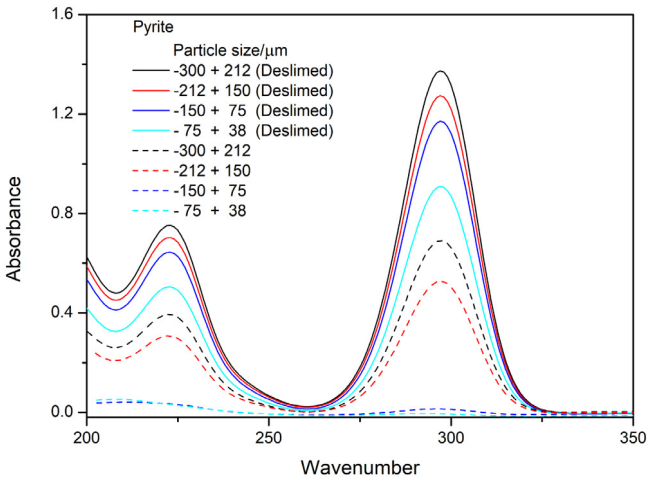

(a)

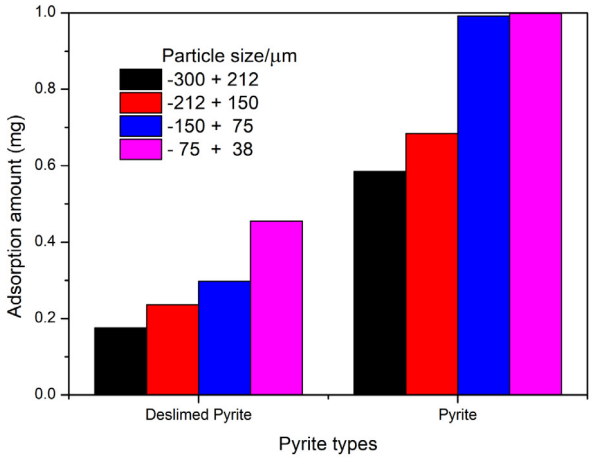

(b)

Fig. 4. UV-visible absorbance of (a) pyrite samples before and after the de-sliming process and (b) their corresponding adsorption amount in 10^{-4} mol/L PAX solution.

PAX adsorbed on the sub-bituminous and meta-bituminous coal samples at various particle sizes in 10^{-4} mol/L PAX solution was determined from the absorbance curves shown in Fig. 3(a) and (b). As shown in Fig. 3(c), the degree of PAX adsorption is low for both coals and does not vary significantly with particle size. Compared with the two coals, as shown in Fig. 4, the adsorption amount of PAX on pyrite for various particle size fractions was much higher. This is because of the expected high chemisorption of PAX on the surface of pyrite particles (Fornasiero and Ralston, 1992a). PAX adsorption increased with decreasing pyrite particle size, which may be attributed to the increase in specific surface area with decreasing particle size (Mathur, 2002). Furthermore, the adsorption amount of PAX on pyrite before and after the de-sliming process showed significant differences. Precisely, PAX adsorption decreased after the de-sliming process for each particle size fraction probably due to the tendency for slimes to adsorb more collector (Mathur, 2002).

In order to further investigate the effect of slimes on the adsorption behaviour of PAX on pyrite, the UV-visible experiments of the sub-bituminous and meta-bituminous coals mixed with

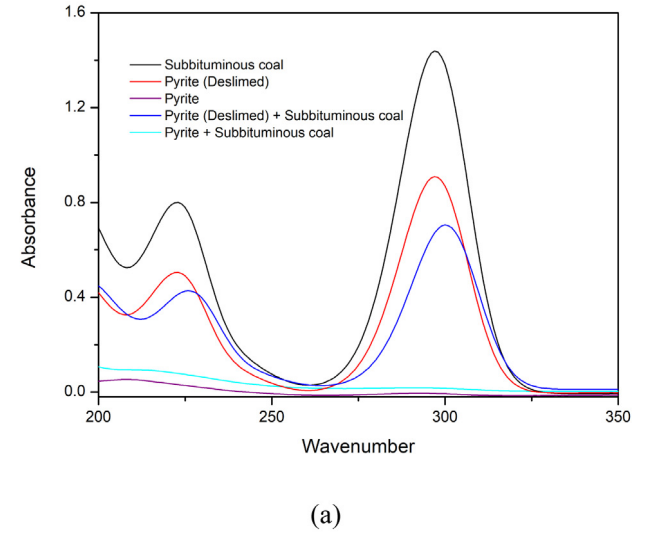

Fig. 5. UV-visible absorbance of (a) sub-bituminous coal (−75 + 45 μm) and (b) meta-bituminous coal (−75 + 45 μm) mixed with pyrite (−74 + 38 μm) before and after de-sliming process, and (c) their corresponding PAX adsorption amount in 10^{-4} mol/L solution.

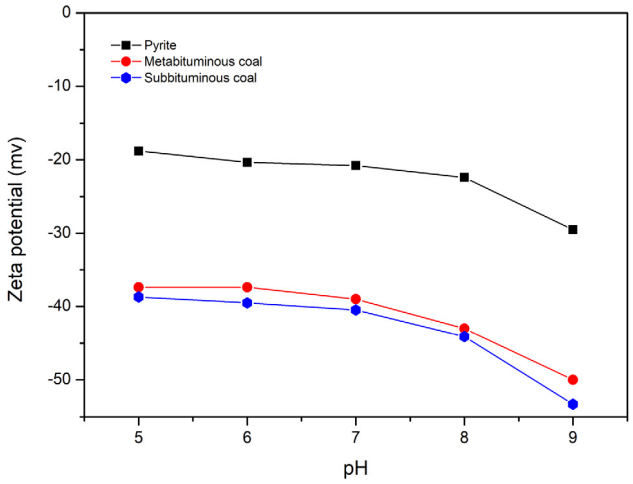

Fig. 6. Zeta potential as a function of pH for sub-bituminous coal, meta-bituminous coal and pyrite in the presence of 10^{-4} mol/L PAX solution.

pyrite were conducted. For this purpose, 0.5 g coal samples (−75 + 45 μm, not de-slimed) with the highest slime content were mixed with pyrite (−74 + 38 μm, either de-slimed or not de-slimed). Fig. 5(a) shows the UV absorbance of sub-bituminous coal and absorbance in the presence of pyrite and deslimed pyrite after PAX addition. Fig. 5(b) shows the PAX absorbance data for meta-bituminous coal. As shown in Fig. 5(c), desliming reduces the adsorption amount of PAX on pyrite by more than 50% because of the removal of fine particles that would otherwise be available for adsorption. The presence of the sub-bituminous or meta-bituminous coal increases the PAX adsorption amount on deslimed pyrite slightly. However, when compared with each other, the PAX adsorption amount on the sub-bituminous and meta-bituminous coal show little difference.

3.3. Zeta potential analysis

The bubble-particle attachment processes during flotation can be significantly impacted by the zeta potential of particles because the charge on particles and bubbles affect the electrostatic interactions with each other. The zeta potential as a function of pH for the sub-bituminous coal, the meta-bituminous coal and pyrite in the presence of 10^{-4} mol/L PAX was shown in Fig. 6. It can be seen that the differences in zeta potential between pyrite, and the sub-bituminous and meta-bituminous coal samples are significant. This indicates that the surface chemistry of pyrite is different from that of the sub-bituminous and meta-bituminous coals, while the two coal samples have a comparable surface charge in the presence of PAX. Pyrite surface is hydrophobic in the presence of PAX due to the chemisorption of xanthate ions and dixanthogen on pyrite surface (Fornasiero and Ralston, 1992b; Valdivieso et al., 2003). It was found in a related study that PAX addition affects the zeta potentials of pyrite more strongly than the two coals (Zhou et al., 2019a). These results suggest that pyrite can be effectively separated from coals in the presence of PAX collector. The zeta potentials of the sub-bituminous and meta-bituminous coals are similar in the presence of PAX most likely due to a similar amount of PAX adsorption on both coals. The literature shows that in similar pH ranges, the zeta potential of air bubbles (measured using micro-electrophoresis method) and the two coals are comparable (Zhou et al., 2019b; Yang et al., 2001). This implies that there is potentially more electrostatic repulsion between bubbles and coal particles than between bubbles and pyrite particles. These observations are in agreement with the UV-visible results.

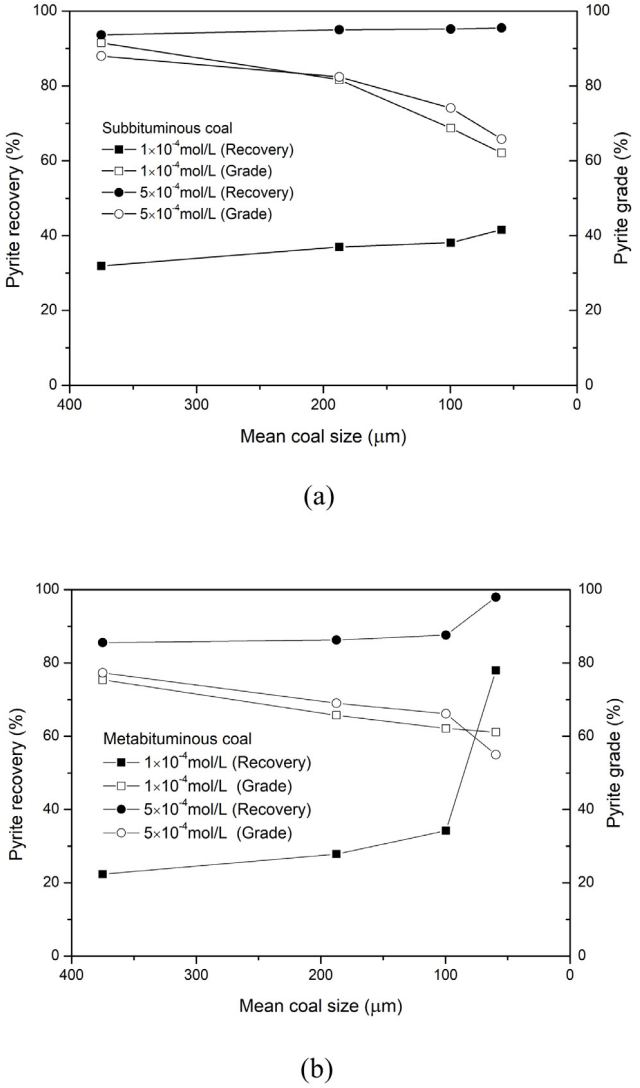

Fig. 7. Pyrite flotation recovery and grade as a function of mean coal particle sizes for (a) sub-bituminous coal and (b) meta-bituminous coal before the de-sliming process. Pyrite particles size −212 + 150 μm, and in the presence of 1×10^{-4} mol/L and 5×10^{-4} mol/L PAX concentration.

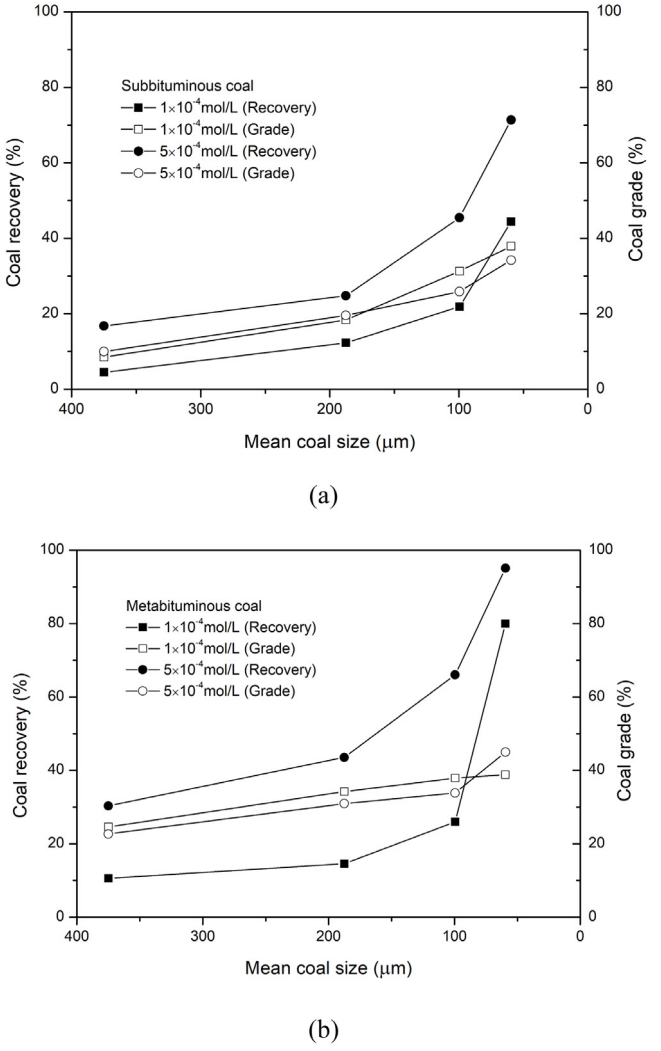

Fig. 8. Coal recovered into the concentrate during flotation of pyrite (−212 + 150 μm) from (a) sub-bituminous coal and (b) meta-bituminous coal before de-sliming process as various coal particle size and PAX concentrations.

3.4. Flotation results

The efficiency in separating pyrite from the sub-bituminous and meta-bituminous coal particles before the de-sliming process were investigated at different coal particle size fractions. Fig. 7(a) and (b) show the flotation recovery and grade of pyrite from the sub-bituminous and of meta-bituminous coals, respectively. In both cases, the recovery of pyrite increases with decreasing particle size while the opposite is true for pyrite grade in the concentrates. The high recovery for pyrite observed for the finer size range in both coals is in good agreement with previous studies which indicate that the maximum pyrite flotation recovery was observed at 50 – 150 μm size range (Trahar and Warren, 1976). Increased detachment of coarse pyrite particles from bubble surfaces is responsible for the low recovery at coarse size (Trahar and Warren, 1976). Fig. 7(a) shows that the recovery of pyrite from sub-bituminous coal increased by 55% when the concentration of PAX increased from 1×10^{-4} mol/L to 5×10^{-4} mol/L. Similarly, pyrite recovery from meta-bituminous coal increased by up to 60% for the coarse size fraction upon increasing PAX concentration from 1×10^{-4} mol/L to 5×10^{-4} mol/L (Fig. 7(b)). The change in pyrite grade with the increase in PAX dosage was insignificant.

As shown in Fig. 8, the recovery and grade of coal in the concentrate during flotation of pyrite from the two coals increased with the decrease of coal particle size for both sub-bituminous and meta-bituminous coals, probably due to the increased entrainment of fine coal particles. By comparison, the recovery of the meta-bituminous coal particles was higher than that of the sub-bituminous coal particles. This is attributed to the higher natural hydrophobicity of the meta-bituminous coal (Xia et al., 2015b). Additionally, the recovery of coal increased with an increase in PAX concentration. The reason is probably higher entrainment of coal particles at higher PAX concentration.

A comparison of flotation recovery and pyrite grade before and after the de-sliming process were conducted in order to further investigate the influence of slimes on separation efficiency of pyrite from the sub-bituminous and meta-bituminous coal. As shown in Fig. 9(a), the recovery of pyrite after the de-sliming process was higher than before the de-sliming process for both coals. The effect of de-sliming is particularly significant at lower PAX concentration (1×10^{-4} mol/L) where the pyrite recovery increased by about three-fold. The pyrite recovery increases slightly

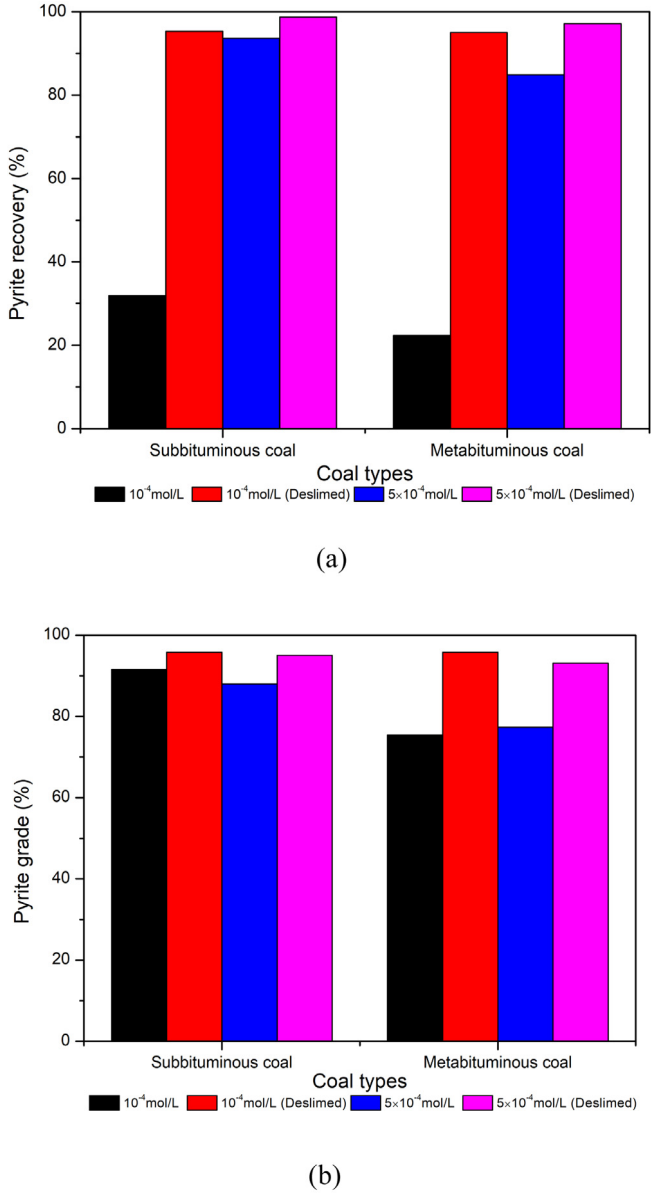

Fig. 9. (a) Pyrite flotation recovery and (b) pyrite grade obtained for pyrite flotation from sub-bituminous and meta-bituminous coal particles before and after de-sliming at different PAX concentrations.

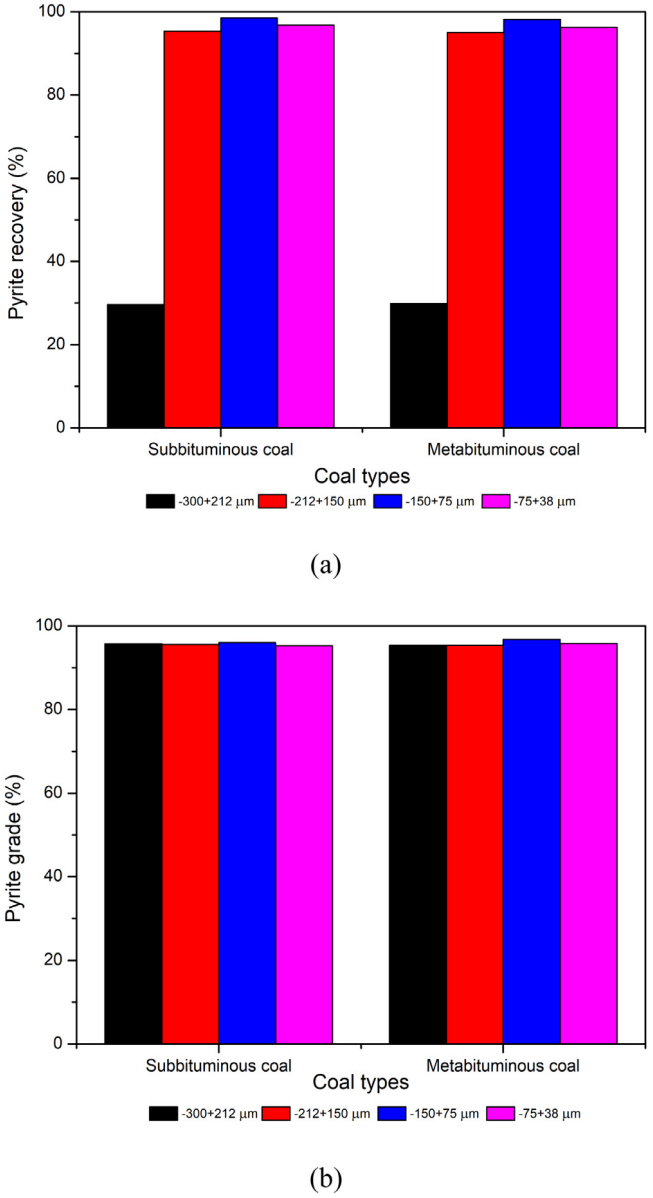

Fig. 10. (a) Pyrite flotation recovery and (b) pyrite grade during flotation in sub-bituminous and meta-bituminous coal particles after the de-sliming process with different pyrite particle size fractions in 1×10^{-4} mol/L PAX solution.

after the de-sliming process in 5×10^{-4} mol/L PAX solution for both the sub-bituminous and meta-bituminous coals. Interestingly, the de-sliming process appears to have a higher impact on pyrite grade (increased by $>$ 20%) in the meta-bituminous coal in comparison with that in the sub-bituminous coal as shown in Fig. 9(b). This occurs probably due to higher nature hydrophobicity of the meta-bituminous coal than the sub-bituminous coal.

The effect of pyrite particle size on its separation efficiency from the sub-bituminous and meta-bituminous coal ($-500 + 250$ μm) after the de-sliming process was studied in 1×10^{-4} mol/L PAX solution. As can be seen in Fig. 10(a), the flotation recoveries for all pyrite particle size fractions except $-300 + 212$ μm were high after the de-sliming process. The reason for poor recovery at the coarsest size fraction could be attributed to the relatively high density of pyrite particles (around 5.0 g/cm^3) becoming a limiting factor. In contrast, due to the lower density of coal particles (around 1.5 g/cm^3), the upper size limit for coal flotation can be as large as 500 μm (Xia et al., 2014; Wang et al., 2016). Interestingly, pyrite grade was found to be independent of particle size and coal rank as shown in Fig. 10(b). The above flotation results indicate that the presence of slimes affects flotation through high collector consumption and entrainment.

4. Conclusions

The effects of slimes and particle sizes of coal and pyrite on the separation of pyrite from the sub-bituminous and meta-bituminous coals were studied. The flotation of pyrite using PAX collector was conducted to establish the limitations of the de-sliming process on pyrite recovery and grade. For the coal particle size, considered in this study, the recovery of pyrite from the sub-bituminous coal and meta-bituminous coal before de-sliming increased by 55% and 60%, respectively, when the concentration of PAX increased from 1×10^{-4} mol/L to 5×10^{-4} mol/L. The UV–Vis analysis revealed a 50% higher amount of PAX adsorption

on particles in the presence of slimes as compared with that after the de-sliming process, possibly due to higher surface area of slimes. However, for the PAX concentration range, used in this study, the recovery of pyrite from the meta-bituminous coal increased by 20%, and that from the sub-bituminous increased by 10% after the de-sliming process. The flotation recovery of pyrite increased with decreasing both pyrite and coal particle sizes when the feed was de-slimed. The sub-bituminous coal recovery of 72% and the meta-bituminous coal recovery of 95% were observed during pyrite flotation from $-74 + 45$ μm coal size fraction at PAX concentration of 5×10^{-4} mol/L. This suggests that desulphurization of fine coals is more challenging probably due to the increased entrainment of fine coal particles during pyrite flotation.

Acknowledgements

This work was supported by the National Key R&D Program of China (Grant No. 2018YFC0604702), the National Natural Science Foundation of China (Grant No. 51804305), and the Natural Science Foundation of Jiangsu Province of China (Grant No. BK20180656).

References

Agorhom, E.A., Skinner, W., Zanin, M., 2014. Diethylenetriamine depression of Cu-activated pyrite hydrophobised by xanthate. Miner. Eng. 57, 36–42.
Akcil, A., Koldas, S., 2006. Acid Mine Drainage (AMD): causes, treatment and case studies. J. Cleaner Prod. 14 (12–13), 1139–1145.
Çınar, M., 2009. Floatability and desulfurization of a low-rank (Turkish) coal by low-temperature heat treatment. Fuel Process. Technol. 90 (10), 1300–1304.
Chen, S., Tang, L., Tao, X., Chen, L., Yang, Z., Li, L., 2017a. Effect of oxidation processing on the surface properties and floatability of meizhiyou long-flame coal. Fuel 210, 177–186.
Chen, S., Yang, Z., Chen, L., Tao, X., Tang, L., He, H., 2017b. Wetting thermodynamics of low rank coal and attachment in flotation. Fuel 207, 214–225.
Demirbas, A., Balat, M., 2004. Coal desulfurization via different methods. Energy Sour. 26, 541–550.
Dou, D., Yang, J., Liu, J., Zhang, H., 2015. A novel distribution rate predicting method of dense medium cyclone in the Taixi coal preparation plant. Int. J. Miner. Process. 142, 51–55.
Eligwe, C.A., 1988. Microbial desulphurization of coal. Fuel 67, 451–458.
Fiedler, R., Bendler, D., 1992. ESCA investigations on Schleenhain lignite lithotypes and the hydrogenation residues. Fuel 71 (4), 381–388.
Fornasiero, D., Ralston, J., 1992a. The interaction of ethyl xanthate with pyrite. Electrochem. Miner. Met. Process. 191–220.
Fornasiero, D., Ralston, J., 1992b. Iron hydroxide complexes and their influence on the interaction between ethyl xanthate and pyrite. J. Colloid Interface Sci. 151 (1), 225–235.
Fuerstenau, D.W., Diao, J., Hanson, J.S., 1990. Estimation of the distribution of surface sites and contact angles on coal particles from film flotation data. Energy Fuels 4, 34–37.
Fuerstenau, M.C., Jameson, G.J., Yoon, R., 2007. Froth flotation: a century of innovation. SME.
Fuerstenau, D.W., Yang, G., Laskowski, J.S., 1987. Oxidation phenomena in coal flotation part I. Correlation between oxygen functional group concentration, immersion wettability and salt flotation response. Coal Prep. 4 (3–4), 161–182.
Ga Siorek, J., 1997. Waste pyritic coal as a raw material for energetic industry. Fuel Process. Technol. 52 (1–3), 175–182.
Jha, R.K.T., Satur, J., Hiroyoshi, N., Ito, M., Tsunekawa, M., 2011. Suppression of floatability of pyrite in coal processing by carrier microencapsulation. Fuel Process. Technol. 92 (5), 1032–1036.
Kawatra, S.K., Eisele, T.C., 1997. Pyrite recovery mechanisms in coal flotation. Int. J. Miner. Process. 50 (3), 187–201.
Kumar, S., Venugopal, R., 2017. Performance analysis of jig for coal cleaning using 3D response surface methodology. Int. J. Mining Sci. Technol. 27 (2), 333–337.
Mathur, S., 2002. Kaolin flotation. J. Colloid Interface Sci. 256 (1), 153–158.
Mukerjee, A., Mukerjee, P., 1962. Spectrophotometric analysis of long chain amines by a dye extraction method. J. Appl. Chem. 12 (3), 127–129.
Ni, C., Bu, X., Xia, W., Peng, Y., Xie, G., 2018. Effect of slimes on the flotation recovery and kinetics of coal particles. Fuel 220, 159–166.
Oats, W.J., Ozdemir, O., Nguyen, A.V., 2010. Effect of mechanical and chemical clay removals by hydrocyclone and dispersants on coal flotation. Miner. Eng. 23 (5), 413–419.
Tang, L., 2017. Characteristics of fluidization and dry-beneficiation of a wide-size-range medium-solids fluidized bed. Int. J. Mining Sci. Technol. 27 (3), 467–471.
Trahar, W.J., Warren, L.J., 1976. The flotability of very fine particles - a review. Int. J. Miner. Process. 3, 103–131.
Valdivieso, A.L., Escamilla, C.O., Song, S., Baez, I.L., Martinez, I.G., 2003. Adsorption of isopropyl xanthate ions onto arsenopyrite and its effect on flotation. Int. J. Miner. Process. 69 (1–4), 175–184.
Wang, B., Peng, Y., Vink, S., 2013. Diagnosis of the surface chemistry effects on fine coal flotation using saline water. Energy Fuels 27 (8), 4869–4874.
Wang, Y., Xing, Y., Gui, X., Cao, Y., Xu, X., 2016. The characterization of flotation selectivity of different size coal fractions. Int. J. Coal Prep. Util. 38 (7), 337–354.
Wang, Y., Zhou, Y., Yang, J., 2017. Structure and optimization of a two-stage equal-density dense medium cyclone. Energy Fuels 31 (7), 7662–7672.
Xia, W., Ren, C., Peng, Y., Pan, D., 2015a. Comparison of traditional and zero-conditioning flotation performances of oxidized anthracite coal. Powder Technol. 275, 280–283.
Xia, W., Ren, C., Peng, Y., Pan, D., 2015b. Comparison of traditional and zero-conditioning flotation performances of oxidized anthracite coal. Powder Technol. 275 (9), 280–283.
Xia, W., Xie, G., Liang, C., Yang, J., 2014. Flotation behavior of different size fractions of fresh and oxidized coals. Powder Technol. 267, 80–85.
Xia, W., Xie, G., Peng, Y., 2016. Comparison of flotation performances of intruded and conventional coals in the absence of collectors. Fuel 164, 186–190.
Xia, W., Yang, J., 2013. Reverse flotation of Taixi oxidized coal. Energy Fuels 27 (12), 7324–7329.
Yang, C., Dabros, T., Li, D., Czarnecki, J., Masliyah, J.H., 2001. Measurement of the zeta potential of gas bubbles in aqueous solutions by microelectrophoresis method. J. Colloid Interface Sci. 243, 128–135.
Ye, Y., Jin, R., Miller, J.D., 1988. Thermal treatment of low-rank coal and its relationship to flotation response. Coal Prep. 6 (1–2), 1–16.
Zhou, Y., Albijanic, B., Tadesse, B., Wang, Y., Yang, J., Li, G., Zhu, X., 2019a. Flotation behavior of pyrite in sub-bituminous and meta-bituminous coals with starch depressant in a microflotation cell. Fuel Process. Technol. 187, 1–15.
Zhou, Y., Albijanic, B., Tadesse, B., Wang, Y., Yang, J., Li, G., Zhu, X., 2019b. Surface hydrophobicity of sub-bituminous and meta-bituminous coal and their flotation kinetics. Fuel 242, 416–424.